Confinement and Surface Effects on the Molecular Dynamics of a Nematic Mixture Investigated by Dielectric Relaxation Spectroscopy

A. R. Brás,[†] M. Dionísio,[†] and A. Schönhals*[,‡]

REQUIMTE, Departamento de Química, Faculdade de Ciências e Tecnologia, Universidade Nova de Lisboa, 2829-516 Caparica, Portugal, and Federal Institute of Materials Research and Testing (BAM), Unter den Eichen 87, D-12205 Berlin, Germany

Received: March 11, 2008; Revised Manuscript Received: April 15, 2008

Broadband dielectric spectroscopy ($10^{-2}-10^{9}$ Hz) was employed to investigate the molecular dynamics of the liquid crystalline mixture E7 confined in both untreated and lecithin-treated 20 nm Anopore membranes. Because E7 does not crystallize, it was possible to cover a temperature range of more than 200 K, providing an exhaustive dielectric characterization of a liquid crystal confined to Anopore membranes for the first time. In the nematic state, the tumbling (α-) and the δ-relaxation are observed, also under confinement conditions. The analysis of their relative intensities give that the orientation of the E7 molecules is preferentially axial in untreated but opposite radial in lecithin-treated pores. The radial alignment of the liquid crystals in the modified membrane is understood as a tail-to-tail conformation of E7 molecules imposed by the adsorbed lecithin molecules. The relaxation rate of the α-process is enhanced for E7 confined in native Anopore compared with the bulk and E7 in treated pores. This is interpreted as resulting from a less dense molecular packing of E7 in the middle of the pore compared to the bulk. In both untreated and treated membranes, the relaxation rate of the δ-process is higher than in the bulk, and the values of the respective Vogel−Fulcher−Tammann temperatures depend on the actual surface treatment. Additionally, a surface process, due to molecular fluctuations of molecules within an adsorbed layer at the pore wall, was detected.

1. Introduction

When a liquid cools down and crystallization can be avoided, a supercooled liquid is obtained. The relaxation times τ of the relevant molecular motions (α-relaxation or dynamic glass transition) slow down dramatically, by 14 orders of magnitude, as temperature is decreased only by a factor of 2. Subsequent cooling to lower temperatures forces the system to freeze in a disordered state to become a glass,[1,2] at the glass transition temperature T_g, usually characterized by a viscosity of 10^{13} Poise, implying a relaxation time exceeding 100 s.[3] Although the phenomena is observed for rather different systems such as polymers, plastic crystals, low molecular-weight glass formers, and silica glasses, the glass transition is not completely understood, remaining at a molecular level as an unsolved problem of the physics of condensed matter.[4] Nevertheless, some universal features are found for all classes of materials, such as the strong temperature dependence of the relaxation time in the supercooled regime characterized by a non-Arrhenius behavior. Close to the glass transition temperature, the temperature dependence of τ can be described by the well-known Vogel−Fulcher−Tammann equation:[5–7]

$$\log \tau = \log \tau_\infty + \frac{A}{T - T_0} = \log \tau_\infty + \frac{(\ln 10)\, DT_0}{T - T_0} \qquad (1)$$

τ_∞ and A are constants, and T_0 is the so-called Vogel temperature. T_0 is found 50−70 K below T_g. The degree of deviation from an Arrhenius-type temperature dependence provides a useful classification of glass formers.[8,9] Materials are called fragile if their $f_p(T)$ dependence deviates strongly from an Arrhenius-type behavior and strong if $f_p(T)$ is close to the latter. Despite of other possibilities, the parameter $D = A/(T_0 \ln 10)$ in eq 1 can be used as quantitative measure of fragility.[8,9]

The most natural explanation of the strong temperature dependence of τ is to assume a cooperative behavior of the relevant molecular motions. The extent of this cooperativity described by a correlation length ξ_α is assumed to increase with decreasing temperature as discussed by Adam and Gibbs the first time.[10] Their theory assumes that the molecular dynamics approaching T_g is controlled by cooperative rearrangements of particles in a so-called cooperatively rearranging region (CRR), which is defined as the smallest number of particles that can change their configuration independently of their neighbors. The volume of a CRR is $V_\alpha = \xi_\alpha$,[3] with ξ_α being the characteristic length scale of the α-relaxation.[11,12] There is some evidence that ξ_α should be in the range of a few nanometers at the glass transition temperature.[13–15] Moreover, there are some experimental results which show the existence of dynamical heterogeneities in glass-forming materials. The typical length scale for these heterogeneities is found again to be in the range of a few nanometers, and their lifetime is in the same order of magnitude as the relaxation time of the α-process close to T_g.[16,17] These findings point to the relevance of a characteristic length scale being responsible for the glass transition.

Studies on molecules confined to porous hosts with dimensions in the nanometer scale can provide indirect information about the relevance of a length scale responsible for glassy dynamics given that ξ_α cannot exceed the pore size.[18] It is well-known that the glass transition is affected when molecules are confined to restricted geometries of nanoscaled size, which tends to lower T_g.[19–22] This is called confinement effect in the literature.[21] Even the α-relaxation can be suppressed for pore

* Corresponding author. E-mail: andreas.schoenhals@bam.de.
† Universidade Nova de Lisboa.
‡ Federal Institute of Materials Research and Testing.

10.1021/jp802133e CCC: $40.75
Published on Web 06/24/2008

sizes lower than a critical value, which allows one to give a minimal length scale for cooperativity.[21] Besides this ideal scenario, molecular dynamics in confining space is also determined by surface effects resulting from interactions of the host system with the guest molecules. These take place at the interface between both, in such a way that when attractive interactions are strong, the value of T_g is actually increased.[21,23] Thus, the glass transition of molecules confined to nanoporous hosts results from a counterbalance between confinement and surface effects.

In liquid crystals (LCs), additional effects such as ordering and phase transition could arise. Moreover, the formation of a surface layer with a partial ordering close to the wall of the host is also discussed.[19] During recent years, LCs were confined to different porous host systems such as porous glasses[24–28] and molecular sieves[29–31] and also to membranes with larger pore sizes[32] like Anopore membranes.[33–36] For the latter cases, the relaxation processes can be only studied in the high-frequency range covering only three orders or magnitude because normally, the LC crystallizes. Therefore, the main effects which are reported in the literature are changes in the orientations of the LC due to confinement. In the present work, dielectric relaxation spectroscopy is applied to study the molecular motions of a nematic liquid crystalline material based mainly on cyanobiphenyl molecules E7, confined to Anopore membranes. E7 was selected for this study because it does not crystallize and shows, besides the isotropic-to-nematic phase transition at $T_{NI} = 333$ K, a glass transition phenomenon with a T_g value of 211 K.[49] Therefore, dielectric spectroscopy can be applied in a broad frequency range from 10^{-2} to 10^9 Hz, covering a temperature range of approximately 200 K, to study whether the relevant molecular motions are modified by the confinement. This was not possible for related cyanobiphenyl systems such as 7OCB[35,37] or 8CB.[36]

Before discussing the particularities induced by the confinement, the details of the molecular dynamics of LCs in the bulk are briefly reviewed. In general, the dielectric relaxation behavior of a liquid crystalline material is different from that of a normal glass former.[38–41] In the isotropic phase, a single dielectric loss peak is observed. By cooling the LC below T_{NI}, the loss peak splits into two processes. Because of the anisotropic structure of the liquid crystalline phase, the dielectric response is related to two main components of the complex dielectric permittivity, $\varepsilon^*_{//}(\omega)$ and $\varepsilon^*_{\perp}(\omega)$, parallel and perpendicular to the nematic director, respectively. Both are due to different weighted sums of four underlying relaxation modes depending on the macroscopic orientation of the sample.[42,43] The relaxation mode with the lowest frequencies is due to rotational fluctuations of the molecule around its short axis. This process determines mainly $\varepsilon^*_{//}(\omega)$ and is called δ-relaxation. The other three relaxation modes (different tumbling motions of the molecules around their long axis) have nearly the same relaxation rate and form one broad relaxation process, which is mostly related to $\varepsilon^*_{\perp}(\omega)$. It is observed at higher frequencies than the δ-process; the intensity of the δ-relaxation relative to that of the tumbling mode depends on the order parameter S of the sample under investigation.

Some controversy exists in the literature concerning which of both relaxation processes detected by dielectric spectroscopy corresponds to glassy dynamics. In a previous work,[44] broadband dielectric and thermal spectroscopy was used to investigate the temperature dependence of both the tumbling and the δ-process in a broad frequency range for bulk E7. It was shown, by comparing dielectric with specific-heat spectroscopy, that the tumbling mode determines the glassy dynamics. For this reason, the tumbling process will be called here α-relaxation, as also introduced by others.[45,46] In this work, DRS studies were performed on E7 confined in a nanoporous inorganic membrane, Anopore, with well-defined and cylindrical ordered pores with a diameter of 20 nm. Both untreated and lecithin-treated Anopore matrices were employed to study surface effects.

2. Experimental Section

The nematic liquid crystal E7 was purchased from Merk (Darmstadt, Germany) and used without further purification. It is a mixture of four components (4-cyano-4′-pentyl-1,1′-biphenyl (51 wt%), 4-*n*-heptyl-4′-cyanobiphenyl (25 wt%), 4,4′-*n*-octyloxycyanobiphenyl (16 wt%), and 4′-*n*-pentyl-4-cyanoterphenyl (8 wt%), see refs 47 and 48) and has the well-known phase transition from the nematic to the isotropic state at $T_{NI} = 333$ K. The glass transition temperature, $T_g = 211$K, was measured by differential scanning calorimetry.[49,50] The dipole moments of the molecules are oriented preferentially to their long axis.

As host for the confinement, porous Anopore membranes were used, supplied by Whatman.[51] They consist of a high-purity Al_2O_3 matrix with pores of 20 nm in diameter. The pores are almost cylindrical trough the membrane with a thickness of 60 μm. The properties of the membranes, such as their large porosity (40% volume), high surface-to-volume ratio, well-defined pore size, and a relatively ordered distribution of pores in the matrix, make them adequate as host material for confinement studies.

Two different sets of samples were investigated with untreated and treated pore surfaces. The samples were prepared in the following way. The Anopore membrane was cut into disks of about 20 mm in diameter. Each disk was outgassed in vacuum of 10^{-4} mbar at 473 K for 12 h to remove water and other impurities. Then, the discs were slowly cooled down to $T =$ 343 K under vacuum. Please, note that this temperature is above the nematic-to-isotropic phase transition of bulk E7. A solution (20 g/L) of E7 in *n*-heptane (PA, Merck) was injected directly into the vacuum chamber. The pores were filled by capillary wetting at that temperature for 72 h. The guest excess and the solvent were removed by a moderate vacuum. The degree of filling was estimated by weighing. By assuming that the density of the LC within the pores is the same as in the bulk state, the amount of the molecules within the pores can be calculated from the porosity (given by the manufacturer) and compared with the experimental data. Each single disk contained 0.7 mg of E7, which supposes an estimated average filling degree of about 96.5%, similar to that obtained by other authors for different LCs.[52,53]

To study the alignment of the LC and its specific surface interaction under confinement, in a second experiment, the pores were treated with a phospholipid from soybean (L-α-lecithin), CAS Number 8002-43-5, obtained by Fluka (Sigma-Aldrich), before filling with E7. The chemical structure of lecithin is given in Figure 1. The native Anopore surface is hydrophilic, providing a strong adsorption for polar headgroup of lecithin. After the high-temperature treatment described above, the disks were cooled down to 273 K under vacuum. A solution of 0.6% w/w of lecithin in hexane (PA, Merck) was injected and allowed to adsorb with the surface of the pores for 4 h. According to the literature, the pore surface should be covered by a monolayer of lecithin molecules by this procedure. Its thickness is estimated to be approximately 2 nm.[54] Then, the rest of the solution was manually removed, and a low vacuum was employed to evaporate the hexane from the pores for 12 h. Two different membranes were prepared in that way. The first one serves as

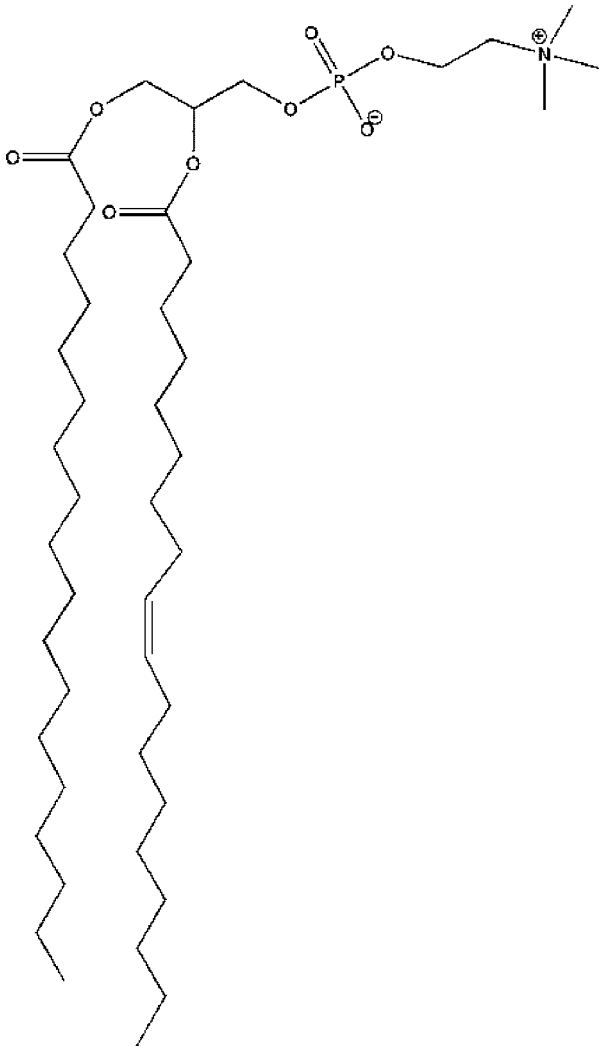

Figure 1. Chemical structure of L-α-lecithin.

blank sample to study only the behavior of the lecithin layer. In the second one, E7 was injected as described above. The filling degree was estimated to be 92.8%. This calculus is based on the assumption that the lecithin amount in the blank sample is the same as that in the specimen filled with E7. Therefore, the volume available for E7 inside the pores was recalculated by subtracting a layer of 2 nm thickness from the pore radius due to the adsorbed lecithin. The filling degree seems to be a bit lower for treated pores, but it is comparable to the value found for native ones.

Finally, a cleaned but empty Anopore membrane is measured for comparison as well.

The equipment to measure the complex dielectric function $\varepsilon^*(f) = \varepsilon'(f) - i\varepsilon''(f)$ (f, frequency; ε', real part, ε'', loss part) from 10^{-2} to 10^9 Hz is described in detail elsewhere.[55] From 10^{-2} to 10^7 Hz, a high-resolution ALPHA analyzer (Novocontrol, Hundsangen, Germany) with an active sample head was used. From 10^6 to 10^9 Hz, a coaxial reflectometer was employed, based on the impedance analyzer HP 4191A. Samples were prepared in parallel-plate geometry between two gold-plated electrodes of 20 and 6 mm diameters. For both setups, isothermal frequency scans were carried out with a temperature stability better than 0.05 K. The temperature was varied from 153 to 411 K, in steps of 2 K, in order to cover both isotropic and nematic phases down to the glass transition temperature of E7.

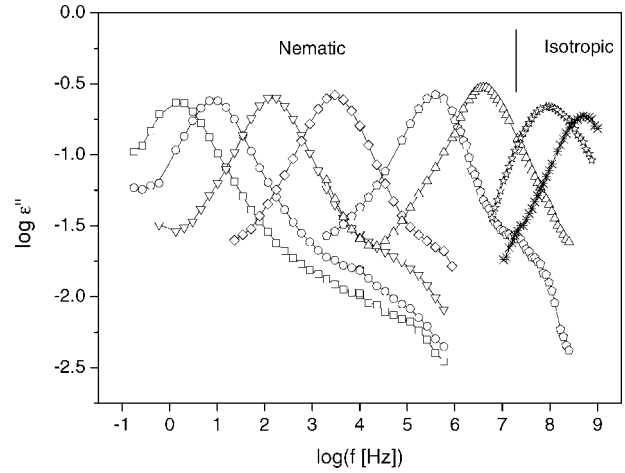

Figure 2. Isothermal dielectric loss spectra for an unaligned sample of E7 confined in untreated Anopore over the frequency range studied and covering both nematic and isotropic states. Nematic state: T = 215 K (□), 219 K (○), 227 K(▽), 239 K (◇), 273 (▲) K, 305 K (Δ). Isotropic state: T = 343 K (☆), 411 K (∗). Lines are guides to the eyes.

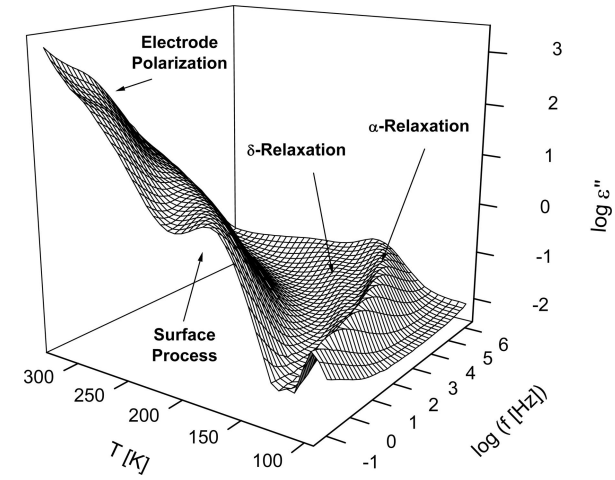

Figure 3. Dielectric loss versus frequency and temperature for E7 confined in a lecithin-treated Anopore membrane in the low-frequency range.

3. Experimental Results and Discussion

Figure 2 presents some isothermal dielectric loss spectra of E7 confined in an untreated Anopore membrane in the available frequency range at temperatures from 215 to 411 K. This figure includes measurements in both the nematic and the isotropic phase. As a first observation, in the nematic state, two peaks are detected, and the most prominent one is associated to $\varepsilon''_{//}(\omega)$, the δ-process. The process mainly associated with $\varepsilon''_{\perp}(\omega)$ (α-process) has a much lower intensity and is located at higher frequencies compared to the δ-relaxation as discussed above.

Both processes merge in a broadened peak for temperatures higher than T_{NI} = 333 K (loss curves presented in Figure 2, at 343 and 411 K). The relative intensities of the δ- and α-relaxation in the nematic range indicate that E7 is mainly axially oriented in the pores; that is, molecules are aligned more or less parallel to the cylindrical pore axis. This means that the nematic director is aligned parallel to the applied electrical field as already observed for bulk E7 on a gold substrate.[44,49]

The complete dielectric spectra of E7 confined to treated pores is given in Figure 3 in a 3D representation versus frequency and temperature. At low temperatures (high frequencies), the

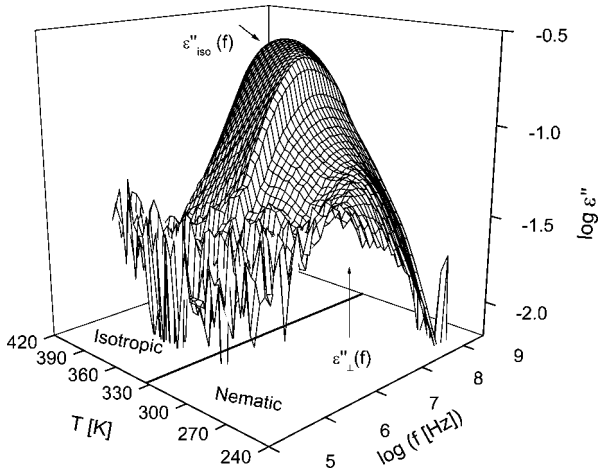

Figure 4. Dielectric loss versus frequency and temperature for E7 confined in a lecithin-treated Anopore membrane in the high-frequency range.

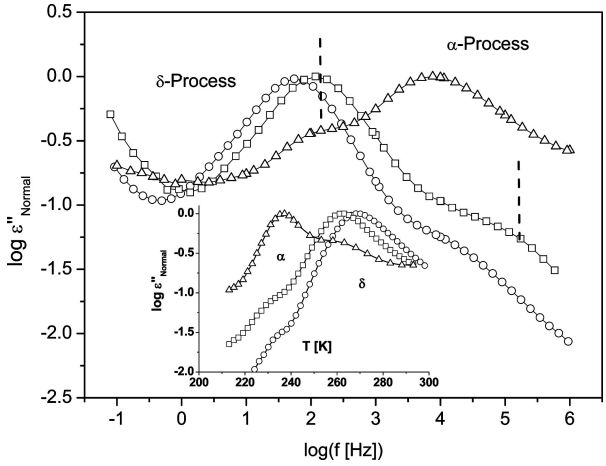

Figure 5. Dielectric loss versus frequency at $T = 227$ K for E7 in the bulk (○), confined to untreated (Δ) and lecithin-treated (□) Anopore membrane. For each sample, the dielectric loss is normalized to its maximum value. Lines are guide to the eyes. The inset gives the dielectric loss versus temperature for the same samples (same symbols) for a fixed frequency of 10^5 Hz. Lines are again guides for the eyes.

already discussed α-relaxation and δ-relaxation are observed. At lowest frequencies and high temperatures, an electrode-polarization phenomenon takes place. Between the electrode polarization and the two above-mentioned loss peaks, an additional dielectric process can be identified as a maximum in the dielectric loss. It is assigned to the fluctuations of an adsorbed surface layer as will be discussed in detail below. Therefore, this process will be called surface process.

To demonstrate that E7 undergoes also in the pores the phase transition from the nematic to the isotropic state, Figure 4 presents the 3D plot of the loss spectra collected in the high-frequency region for E7 embedded into the lecithin-treated Anopore membrane. At the phase transition, the dielectric loss changes dramatically in its frequency and temperature dependence. In the temperature range of the isotropic phase, a single process is observed, as mentioned above. But also for temperatures lower than T_{NI}, only one peak instead of the expected two is detected. Its frequency position seems to be a bit higher than that in the isotropic phase, which might indicate that the process is the α-relaxation.

That leads to the conclusion that the orientation of the molecules is changed in the treated pores compared to the

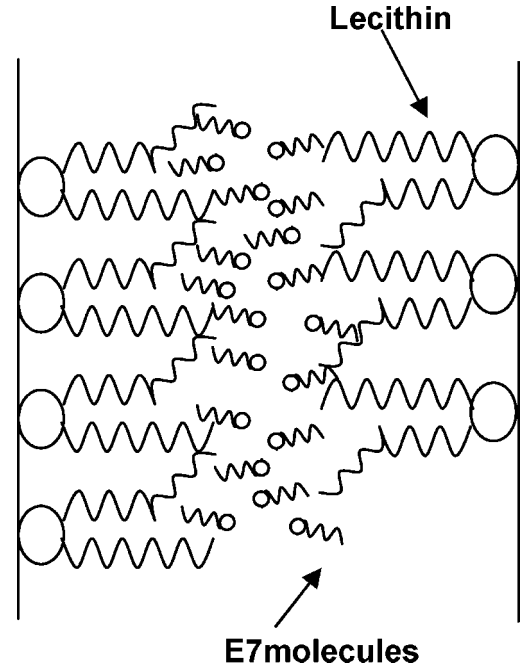

Figure 6. Schematic picture of the E7 molecular arrangement in a lecithin-treated pore; molecules adopt preferentially a radial orientation assuming a tail-to-tail conformation with the hydrophobic lecithin moiety.

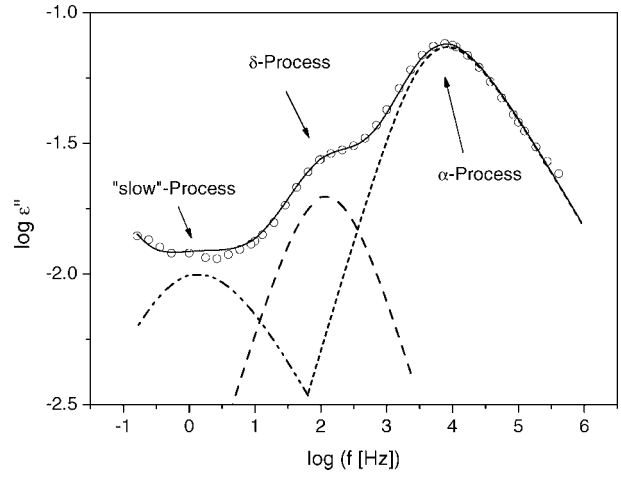

Figure 7. Dielectric loss versus frequency at $T = 227$ K for E7 confined in lecithin-treated Anopore. The solid line is a fit of a sum of three HN-function to the experimental data. The other lines give the contributions of the individual processes to the dielectric loss: dashed-dotted-dotted: slow process; dashed: δ-relaxation; short dashed: α-relaxation.

untreated ones as discussed also in refs 36, 33, and 56. To demonstrate this in more detail, Figure 5 compares the dielectric loss versus frequency for E7 confined to untreated and treated pores at the same temperature together with data for the bulk LC. Because the dielectric losses are quite different in their absolute values, the data are normalized with regard to the corresponding maximum value. The relative dielectric strengths of δ- and α-relaxation are quite similar for bulk E7 and E7 confined to untreated pores. This means, as discussed before, that the dipole moment of the molecules is oriented preferentially parallel to axes of the untreated pores. This is different for E7 embedded in treated Anopore. In this case, the α-relaxation is much stronger in intensity than the δ-process. This leads to the conclusion that for treated pores, the nematic director is preferentially oriented radial to the direction of the pore axis.

The induction of a radial orientation of single component cyanobiphenyl-based LC confined in lecithin-treated pore walls is reported also in refs 25 and 57–59. But for E7 in lecithin-treated Anopore membranes, this is reported here the first time. This becomes also clear when comparing the isochronal data at a frequency of 10^5 Hz versus temperature shown in the inset of Figure 5.

The change of the orientation of E7 molecules can be rationalized by a simple model. The lecithin molecules are anchored to pore surface by the polar headgroup. Therefore, the apolar tails (see Figure 1) are preferentially directed to the pore center. The whole native pore surface is decorated with alkyl chains. When the molecules of E7 are embedded in the modified pores, their apolar tails are forced to orient in a tail-to-tail conformation. This is illustrated schematically in Figure 6.

A closer inspection of Figure 5 shows that also the frequency (or temperature) position of the relaxation processes for confined E7 is shifted in comparison to that for the bulk. This shift depends on the treatment of the pore surfaces. To analyze these findings in more detail, the model function of Havriliak and Negami[60] (HN-function) is fitted to the dielectric spectra. Because multiple peaks are observed in the available frequency window, a sum of HN-functions is used,

$$\varepsilon^*_{\mathrm{Fit}} = \varepsilon_\infty + \sum_j \frac{\Delta\varepsilon_j}{[1+(\mathrm{i}f/f_{0,j})^{\beta_j}]^{\gamma_j}} - \mathrm{i}\frac{\sigma_0}{\varepsilon_0(2\pi f)^s} \qquad (2)$$

where j counts the different relaxation processes. For each process, f_0 is a characteristic frequency related to the frequency of maximal loss $f_p = 1/(2\pi\tau)$ (relaxation rate), and $\Delta\varepsilon$ is the dielectric relaxation strength. β and γ are fractional shape parameters ($0 < \beta \leq 1$ and $0 < \beta\gamma \leq 1$) describing the symmetric and asymmetric broadening of the dielectric spectrum of the considered process. ε_∞ symbolizes the high-frequency limit of the real part $\varepsilon'(f)$ for frequencies much higher than the highest relaxation rate. Conduction effects are treated in the usual way by adding the contribution $\sigma_0/[\varepsilon_0(2\pi f)^s]$ to the dielectric loss, where σ_0 is related to the dc conductivity of the sample and ε_0 is the dielectric permittivity of vacuum. The parameter s ($0 < s \leq 1$) describes for $s = 1$ Ohmic and for $s < 1$ non-Ohmic effects in the conductivity. For details, see ref 61. Figure 7 gives an example of the fitting procedure of three HN-functions to the dielectric spectrum of E7 confined in the lecithin-treated membrane at 227 K. The slow process detected at the lowest frequencies in addition to the δ- and the α-relaxation was also observed for bulk E7,[44,45,49,62] and therefore, it cannot be assigned as originating from a surface layer in confinement (see also refs 31 and 63–65). Its molecular origin is not clear up to now for the bulk as well.

The shape parameters are almost independent of temperature and pore treatment. For the δ-relaxation, a Debye-like behavior ($\beta \approx 1$and $\gamma \approx 1$) is found for both natural and treated pores, as it is already known for the bulk. The α-process has an asymmetric broadened relaxation function ($\beta \approx 0.7$ and $\beta\gamma \approx 0.4$).

The relaxation rates f_p obtained from the fits for the different relaxation processes are plotted versus the inverse of temperature in Figure 8a for E7 confined in untreated and in Figure 8b for E7 confined in lecithin-treated Anopore membranes. The data for bulk E7 are included for comparison (open symbols).

The temperature dependence of the relaxation rates of the slow process seems to be nearly activated, and no influence of the confinement could be detected. Because the molecular origin of this process is not clear up to now, it is not further discussed here.

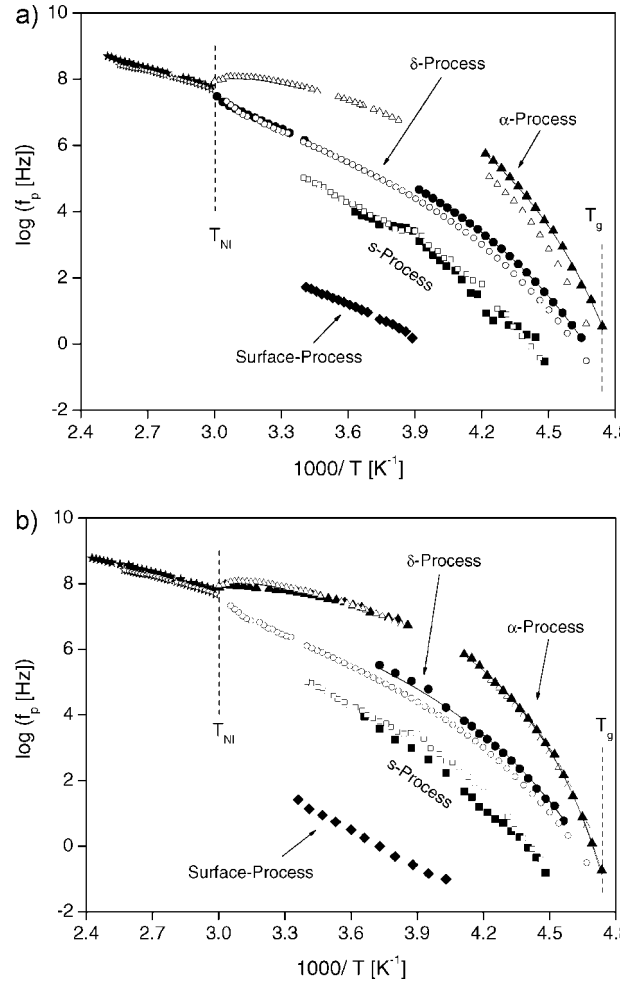

Figure 8. Relaxation rates f_p versus $1/T$ for the different processes for E7 embedded in different pores. The solid symbols corresponds to confined E7, and the open symbols are data for the bulk. Triangles, α-relaxation; circles, δ-relaxation; squares, slow process; diamonds, surface process. The lines are fits of the VFT-equation to the data as described in the text. (a) E7 confined in native pores of the Anopore membrane. (b) E7 confined embedded in lecithin-coated pores of the Anopore membrane.

As it is known for the bulk E7, the temperature dependence of both the α- and the δ-process are curved versus $1/T$ and can be described close to T_g by the VFT-equation (eq 1), also in confinement. For bulk E7, it was found that both dependencies seem to merge close to the glass transition temperature and have quite different Vogel temperatures T_0.[44] The same is true for E7 confined in native and treated Anopore membranes.

Before analyzing the temperature dependence of the relaxation rates in more detail, it is worth pointing out that when the LC is confined in the untreated membrane, the absolute values of the relaxation rates for both the α- and the δ-relaxation are higher than those in the bulk. This means that the confined E7 molecules fluctuate faster compared to the bulk. This is already seen in the raw data (see Figure 5) by the shift of both loss peaks to higher frequencies (or lower temperatures) for confined E7 with respect to the bulk. The magnitude of the discussed effects is within one order of magnitude. When E7 is embedded in lecithin-treated Anopore, the δ-process also shifts to higher frequencies. This is evident from the raw data in the inset of

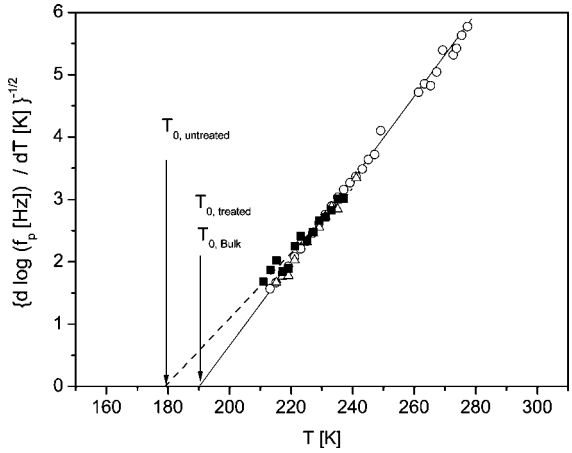

Figure 9. [d log f_p/d T]$^{-1/2}$ versus temperature for the α-process. ○, bulk; ■, untreated pores; △, lecithin-treated pores. Lines are linear regressions to the data. Dashed line, untreated; solid line, bulk and treated.

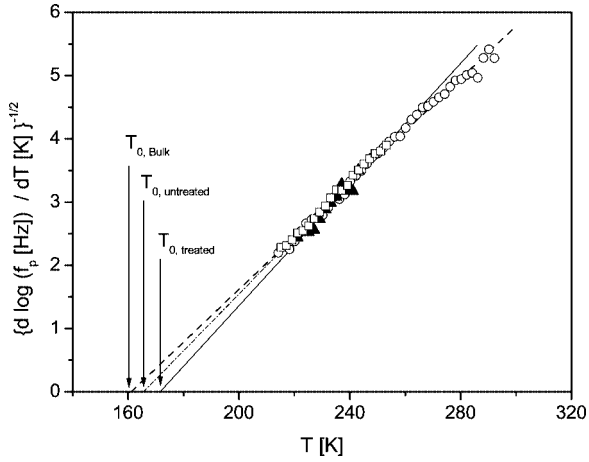

Figure 10. [d log f_p/d T]$^{-1/2}$ versus temperature for the α-process. ○, Bulk; □, untreated pores; ▲, lecithin-treated pores. Lines are linear regressions to the data. Dashed line, bulk; dashed-doted line, untreated; solid line, treated.

Figure 5, where the ε'' maximum of the δ-relaxation is located at lower temperatures relative to the bulk. Nevertheless, no changes seem to occur with regard to the α-relaxation. This will be discussed later on. Also in the isotropic state, the relaxation rate is only barely influenced by the confinement (see Figure 8a,b). Similar findings are reported for different LCs embedded in porous membranes (see ref 21 and references therein).

To analyze the temperature dependencies in more detail a derivative method is used.[66,67] This method is sensitive to the functional form of $f_p(T)$ irrespectively of the prefactor f_∞. For a dependency according to the VFT-equation, one gets

$$\left[\frac{\mathrm{d}\log f_p}{\mathrm{d}T}\right]^{-1/2} = A^{-1/2}(T - T_0) \qquad (3)$$

In a plot [d log f_p/d T]$^{-1/2}$ versus T, a VFT behavior shows up as a straight line. In the following, this method is applied to both the α-relaxation (Figure 9) and the δ-process (Figure 10), where the data for the different confined E7 were compared with the corresponding bulk close to T_g. First, it is concluded that, indeed, for all considered processes, the temperature dependence of the relaxation rates follow the VFT law. All experimental data can be well described by straight lines. But as a second result, the Vogel temperature T_0 is influenced by the confinement. To estimate the parameters of the VFT equation and the fragility D for a quantitative comparison, the following procedure was applied. T_0 and the A parameter were taken from the derivative technique by linear regression. The prefactors were obtained by a fit of the VFT equation to the relaxation rates by keeping T_0 and A fixed. All parameters are collected in Table 1.

TABLE 1: Estimated VFT Parameters for the Different Processes and Samples[a]

sample	$\log_{10}$ (f_∞ [Hz])	T_0 [K]	A [K]	D
	α-Relaxation			
bulk	10.4	190.1	225	2.7
untreated	12.0	179.1	366	4.7
treated	10.3	190.0	236	2.8
	δ-Relaxation			
bulk	10.4	161.0	576	8.2
untreated	10.2	165.0	498	6.9
treated	9.9	171.1	436	5.9

[a] The Vogel temperature and the A parameter were taken from the derivative technique. The prefactors were obtained by a fit of the VFT equation to the relaxation rates by keeping T_0 and A fixed. D was calculated according to eq 1.

Next, the influence of the confinement on the different processes will be discussed:

α-Relaxation. It becomes evident (also from the raw spectra, see Figure 5) that for E7 confined to untreated pores, the relaxation rate is higher than those for the bulk state and for treated pores (see Figure 8a). The data of the latter ones collapse into one chart (see Figure 8b), and the corresponding derivative analysis (see Figure 9) shows that the Vogel or ideal glass transition temperatures are the same, 190 K. T_0 for the α-relaxation of E7 embedded in native pores is lower by 11 K. This is a significant effect (see Table 1). Also, the fragility is higher for the α-relaxation in untreated pores. At a first glance, this might be interpreted as confinement effect, as discussed in the Introduction. But when taking this interpretation, also the data obtained for the treated pores should be affected in a similar way, which is not the case. Moreover, a pore size of 20 nm seems to be too large to cause considerable effects on the α-relaxation.[68,69] In addition, ongoing studies confining E7 to smaller pores provide additional evidence for that conclusion. Therefore, the origin of the lower T_0 for the α-relaxation in untreated pores should be of different nature. For native pores, the polar groups of the molecules of E7 will interact with the pore surface. This increases the density of molecules in a layer close to the surface, leading to a lower dense packing in the middle of the pore than that in the bulk E7. In consequence, the mobility is enhanced, and a lower T_0 is observed. For treated pores, the guest molecules do not interact directly with the surface, and therefore, a behavior similar to that in the bulk is observed.

***δ*-Relaxation.** The relaxation rates of the δ-process in both native and lecithin-treated pores are higher than those in the bulk (see Figure 8). The respective derivative plot (see Figure 10) gives that also the Vogel temperature and fragility vary systematically with the treatment of the pores. The lowest Vogel temperature is found for bulk E7, followed by that of E7 in untreated pores. For the δ-relaxation of E7 confined to treated pores, a 10 K higher value of T_0 is obtained compared to the bulk (see Table 1). This is again a significant effect. The origin of the δ-relaxation is rotational fluctuations of the molecules around their short axis. The length scale of the involved molecular fluctuations should be larger than that of the

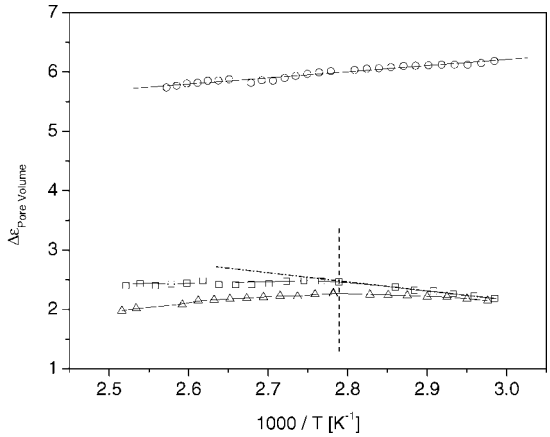

Figure 11. $\Delta\varepsilon$ normalized to the pore fraction versus inverse temperature for temperatures higher than $T_{N/I}$. ○, bulk; □, untreated pores; Δ, lecithin-treated pores. Lines are guides for the eyes. The dashed-dotted line indicates the increase of $\Delta\varepsilon$ at lower temperatures for E7 confined to untreated pores.

α-process. Therefore, this relaxation process is more sensitive to surface interaction than the former one.

Dielectric Relaxation Strength. The absolute values of the dielectric relaxation strengths for the α- and δ-relaxation depend on the orientation of the molecules. For the confined E7, the orientation of the molecules cannot be quantified. Therefore, here, only the dielectric strengths, $\Delta\varepsilon$, in the isotropic range which do not depend on the orientation are compared. The values are normalized with respect to the pore volume fraction (Figure 11). The Debye theory of dielectric relaxation generalized by Kirkwood and Fröhlich[70] predicts the following equation for the temperature dependence of the dielectric relaxation strength,

$$\Delta\varepsilon = \frac{1}{3\varepsilon_0} g \frac{\mu^2}{k_B T} \frac{N}{V} \tag{4}$$

where μ is the mean dipole moment of the moving unit that relaxes with the under consideration and N/V is the number density of dipoles involved. g is the so-called Kirkwood/Fröhlich correlation factor which describes static correlation between the dipoles. k_B is the Boltzmann constant. The Onsager factor describing internal field effects is omitted for sake of simplicity.

The dielectric strength for bulk E7 is higher than that for confined E7 by a factor of approximately 3. According to eq 4, this means that a large fraction of molecules do not contribute to that relaxation process at these temperatures and frequencies. These molecules strongly interact with the surface and are slowed down in their mobility or become completely immobilized, which will be discussed later. Moreover, the temperature dependency for confined E7 is different in confinement than in the bulk. For the latter, $\Delta\varepsilon$ decreases with $1/T$ as expected. For confined E7, $\Delta\varepsilon$ first increases slightly up to a certain temperature and than decreases with further increase of temperature. This can be understood by assuming two competing effects. On the one hand, the thermal energy k_BT increases with increasing temperature. This would lead to a decrease of $\Delta\varepsilon$ according to eq 4. On the other hand, because of a reduced interaction, the adsorbed molecules become more mobile with increasing temperatures. This can be expressed by a growing number density of contributing dipoles. Therefore, for lower temperatures, the increase of the dipole density overcompensates the influence of the thermal energy. At higher temperatures, the thermal energy wins, although the decrease in $\Delta\varepsilon$ is still smaller than that in the bulk.

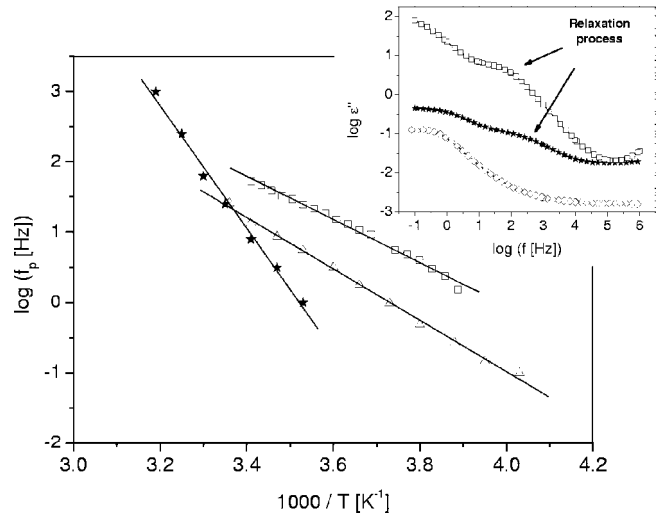

Figure 12. Relaxation rate f_p versus $1/T$ for the surface process. ★, lecithin layer; Δ, E7 in lecithin-coated pores; □, E7 in native pores. Lines are fits of the Arrhenius equation to the data. The inset gives the dielectric loss versus frequency at $T = 303$ K for an empty Anopore membrane (◇), pores coated with a lecithin layer, and E7 in lecithin-treated ◇. Lines are guides for the eyes.

There are also differences between the temperature dependence of $\Delta\varepsilon$ for E7 confined to native and treated pores. For E7 confined to native pores, $\Delta\varepsilon$ is more or less constant, whereas $\Delta\varepsilon$ for E7 confined to treated pores decreases. To understand this, one has to keep in mind that for native pores, the E7 molecules, which are monitored by dielectric spectroscopy, directly interact with the surface (hard interface), whereas for treated pores, the lecithin molecules are between the hard pore walls and the E7 (soft interface). For this reason, the increase in the dipole density with temperature is stronger for E7 embedded in native pores than for treated pores, because in the latter case, the E7 molecules are already more decoupled from/less anchored on the surface. This results in a stronger decrease of $\Delta\varepsilon$ with increasing temperature for lecithin-treated pores.

Surface Relaxation. Figure 3 shows that there is an additional process located at lower frequencies than those of the α- and δ-process. At a first glance, that might be due to a Maxwell/Wagner/Sillars polarization. Such a phenomenon is related to the blocking of charge carriers at interfaces, as observed for nanoporous hosts.[71] But in the experiment presented here, the cylindrical pores are perfectly oriented in the direction of the electrical field that drives the charge carriers. Therefore, the probability of the blocking of charge carriers is low. But the analysis of the relaxation strength gives that a considerably amount of molecules are in close interaction with the surface. As a consequence, the molecular mobility of these molecules is slowed down. Therefore, the fluctuations of part of these molecules should be observed by dielectric spectroscopy at higher temperatures and lower frequencies. Therefore, the relaxation process observed at lower frequencies than those of the α- and δ-process is assigned to molecules which are slowed down because of the interaction with the surface.

To confirm this interpretation, measurements for an empty and a lecithin-coated Anopore membrane were carried out. For $T = 303$ K, the dielectric loss is compared for the empty, the blank lecithin-coated, and E7 in treated pores in the inset of Figure 12. For the empty Anopore, besides an electrode polarization, no dielectric active process is observed. In contrast to the empty membrane, a further relaxation process is observed for the lecithin-modified membrane. Because the only difference

with the empty membrane is the lecithin layer, this process is assigned to fluctuations of the adsorbed lecithin molecules in that surface layer. NMR studies confirm the existence of molecular motions in close packed adsorbed lechitin such as reorientational fluctuations with the polar headgroup fixed at the pore surface.[54] For the E7 filled lecithin-treated membrane, the surface process discussed above is observed at nearly the same frequency position. This coincidence gives further evidence that this assignment seems to be correct.

The processes are also analyzed by fitting the HN-function to the data. Because of the electrode polarization phenomena, only the relaxation rate can be estimated (see Figure 12). Their temperature dependencies seem to be linear with $1/T$, and an apparent activation E_A can be estimated. For the membrane coated only with the lecithin layer, a rather high value of 166 kJ/mol is obtained. This points to a strong adsorption of the lecithin molecules on the pore walls of the Anopore membrane. For E7 confined to the Anopore membrane, lower values are obtained, which depend on the surface treatment: 70 kJ/mol for lecithin-treated pores and 59 kJ/mol for native pores. It is worth noting that the value estimated for treated pores is between that calculated for native and that for the single lecithin-coated pores. Obviously, the strongly adsorbed lecithin molecules have a considerable impact on the molecular fluctuations of the near-surface E7 molecules. This is also in agreement with the observation that the highest value of the Vogel temperature is observed for treated pores.

4. Conclusions

Broadband dielectric relaxation spectroscopy was employed for the first time to investigate the molecular dynamics of a nematic liquid crystal, E7, confined to both native and lecithin-treated pores of Anopore membranes. A wide temperature range was used to cover the isotropic-to-nematic phase transition down to the glass transition temperature.

Besides the relaxation peak characteristic for the isotropic state (above 333 K), two main relaxation processes were detected in the nematic range, labeled as α- and δ-relaxation in order of decreasing frequency. The former process is related to molecular tumbling modes, and the latter is due to rotational fluctuations around the molecular short axis of the molecules. The relative intensities of the both relaxation processes are directly related to the orientation of the nematic director with respect to measuring electrical field. Both the alignment and the molecular mobility of E7 are influenced by the confinement and the treatment of the pore surfaces. In the first case, when the LC is confined to the native pores of the membrane, the dominating relaxation process is the δ-relaxation, which corresponds to a preferential alignment of the nematic director parallel to the electric field. Because the pores are also parallel to the field, this is an indication that E7 molecules are mainly orientated with their long axis tangential to the pore axis. In the other case, when E7 is confined to the modified membrane, the prominent peak is due to the α-relaxation, corresponding to a perpendicular alignment of the nematic director with respect to the outer field. This means that the long axis of the molecules is arranged in a radial orientation perpendicular to the pore axis. The change in orientation was rationalized by a special arrangement of the E7 molecules as embedded in the modified pores with their apolar tails forced to adopt a tail-to-tail conformation with the hydrophobic lecithin alkyl groups.

The temperature dependence of the relaxation rates of both the δ- and the α-process follows the VFT equation. The relaxation rate of the latter is higher by around 1 order of magnitude when E7 is confined to untreated pores of the Anopore membrane. A derivative method was applied to estimate the VFT parameters, especially the Vogel temperature T_0. For the α-relaxation, a T_0 value 11 K lower than that for the bulk is found. This is a significant effect which, however, cannot be attributed to a confinement effect, as discussed in the Introduction. A more reasonable explanation assumes a different dynamical nature of the α-relaxation, which is also supported by a change in the fragility index. The higher relaxation rate can be interpreted in terms of a lower density of E7 in the pore center relative to that in the pore wall where the molecules are anchored in a dense packing arrangement. In the treated pores of the Anopore membrane, a lecithin layer is already settled at the pore wall and the E7 molecules behave similarly to the bulk state with regard to the α-relaxation, leaving its relaxation rate unaffected.

For confined E7, either in native or modified pores of the Anopore membrane, the relaxation rate is enhanced about 1 order of magnitude for the δ-process, and T_0 decreases with surface treatment. The higher length scale involved in this process relatively to that of the α one makes it more sensitive to surface interactions.

The temperature dependence of the relaxation rates of the relaxation process observed in the isotropic state is only barely influenced by the confinement. The main effect is a considerable reduction of the dielectric relaxation strength, which is explained by a relatively high amount of molecules which are immobilized at the pore walls or slowed down in their molecular mobility.

In addition to the α- and the δ-relaxation at lower frequencies, a so-called surface relaxation process is observed. This relaxation process is assigned to molecules which are in close or even strong interaction with the pore surface. The temperature dependence of the corresponding relaxation rates can be described by an Arrhenius law with an apparent activation energy E_A. The highest value of E_A is found for the lecithin-treated unfilled pores, followed by that of E7 in treated pores. The lowest E_A is found for the LC-confined native pores. This is discussed in terms of the different interaction of the molecules with the pore wall.

Acknowledgment. The authors acknowledge the financial support to Fundação para a Ciência e Tecnologia through Projects POCTI/CTM/47363/2002, PCTD/CTM/64288/2006, and FEDER. A.R.B. also thanks Fundação para a Ciência e Tecnologia for the PhD Grant SFRH/BD/23829/2005 and the Federal Institute of Materials Research and Testing (BAM) for the use of its research facilities.

References and Notes

(1) Stickel, F.; Fischer, E. W.; Richert, R. *J. Chem. Phys.* **1995**, *102*, 6251.
(2) Jäckle, J. *Rep. Prog. Phys.* **1986**, *49*, 171.
(3) *Disorder Effects on Relaxational Processes*; Richert R., Blumen A. Eds.; Springer: Berlin, 1994.
(4) (a) Anderson, P. W. *Science* **1995**, *267*, 1615. (b) Angel, C. A. *Science* **1995**, *267*, 1924.
(5) Vogel, H. *Phys. Zeit.* **1921**, *22*, 645.
(6) Fulcher, G. S. *J. Am. Ceram. Soc.* **1925**, *8*, 339.
(7) Tammann, G.; Hesse, G. *Anorg. Allgem. Chem.* **1926**, *156*, 245.
(8) Angell, C. A. *J. Non-Cryst. Solids* **1991**, *13*, 131.
(9) Angell, C. A. J. *Res. Natl. Inst. Stand. Technol.* **1997**, *102*, 171.
(10) Adams, G.; Gibbs, J. H. *J. Chem. Phys.* **1965**, *43*, 139.
(11) Donth, E.; Huth, H.; Beiner, M. *J. Phys.: Condens. Matter* **2001**, *13*, L451.
(12) Beiner, M. *Macromol. Rapid Commun.* **2001**, *22*, 869.
(13) Donth, E.; Huth, H.; Beiner, M. *J. Phys.: Condens. Matter* **2001**, *13*, L451.
(14) Donth, E. *The Glass Transition*; Springer Verlag: Berlin, 2001.

(15) Fischer, E. W.; Donth, E. J.; Steffen, W. *Phys. Rev. Lett.* **1992**, *68*, 2344.
(16) Sillescu, H. *J. Non-Cryst. Solids* **1999**, *243*, 81.
(17) Ediger, M. D. *Annu. Rev. Phys. Chem.* **2000**, *51*, 99.
(18) Schönhals, A.; Goering, H.; Schick, Ch.; Frick, B.; Zorn, R. *J. Non-Cryst. Solids* **2005**, *351*, 2668.
(19) Aliev, F. M. *Liquid Crystals and Polymers in Pores, The influence of Confinement on Dynamic and Interfacial Properties*; Crawford, G. F., Zŭmer, S. Eds.; Taylor and Francis: London, 1996.
(20) Kranbuehl, D.; Knowles, R.; Hossain, A.; Hurt, M. *J. Phys.: Condens. Matter* **2003**, *15*, S1019.
(21) Kremer, F.; Huwe, A.; Schönhals, A.; Różański, S. A. Molecular Dynamics in Confining Space. In *Broadband Dielectric Spectroscopy*; Schönhals, A.; Kremer, F. Eds.; Springer Verlag: Berlin, 2003.
(22) Leys, J.; Sinha, G.; Glorieux, C.; Thoen, J. *Phys. Rev. E* **2005**, *71*, 051709.
(23) Schönhals, A.; Goering, H.; Schick, Ch. *J. Non-Cryst. Solids* **2002**, *305*, 140.
(24) Aliev, F.; Sinha, G. *Mol. Cryst. Liq. Crys.* **2001**, *364*, 435.
(25) Sinha, G.; Leys, J.; Glorieux, C.; Thoen, J. *Phys. Rev. E* **2005**, *72*, 051710.
(26) Cramer, Ch.; Cramer, Th.; Kremer, F.; Stannarius, R. *J. Chem. Phys.* **1997**, *106*, 3730.
(27) Massalska-Arodź, M.; Krawczyka, J.; Procyk, B.; Kremer, F. *Phase Transitions* **2007**, *80*, 687.
(28) Werner, J.; Otto, K.; Enke, D.; Pelzl, G.; Janowski, F.; Kresse, H. *Liq. Cryst.* **2000**, *10*, 1295.
(29) Frunza, S.; Frunza, L.; Schönhals, S. *J. Phys. IV France* **2000**, *10*, 115.
(30) Frunza, L.; Kosslick, H.; Frunza, S.; Schönhals, A. *Microporous Mesoporous Mater.* **2006**, *90*, 259.
(31) Frunza, S.; Frunza, L.; Schönhals, A.; Zubowa, H. L.; Kosslick, H.; Carius, H. E.; Frick, R. *Chem. Phys. Lett.* **1999**, *307*, 167.
(32) Rózanski, S. A.; Stannarius, R.; Kremer, F.; Diele, S. *Liq. Cryst.* **2001**, *28*, 1071.
(33) Rózanski, S. A.; Kremer, F.; Groothues, H.; Stannarius, R. *Mol. Cryst. Liq. Crys.* **1997**, *303*, 319.
(34) Nazario, Z.; Sinha, G. P.; Aliev, F. M. *Mol. Cryst. Liq. Crys.* **2001**, *367*, 333.
(35) Diez, S.; Pérez-Jubindo, M. A.; De la Fuente, M. R.; López, D. O.; Salud, J.; Tamarit, J. L. *Chem. Phys. Lett.* **2006**, *423*, 463.
(36) Bengoechea, M. R.; Aliev, F. M. *J. Non-Cryst. Solids* **2005**, *351*, 2685.
(37) Diez, S.; López, D. O.; De la Fuente, M. R.; Pérez-Jubindo, M. A.; Salud, J.; Tamarit, J. L. *J. Phys. Chem. B* **2005**, *109*, 23209.
(38) Kremer, F.; Schönhals, A. Molecular and Collective Dynamics of Polymeric. Liquid Crystals. In *Broadband dielectric Spectroscopy*; Kremer, F., Schönhals, A. Eds.; Springer Verlag: Berlin, 2003; pp 392 ff.
(39) Moscicki, J. K. *Liquid crystal polymers - from structure to application*; Collyer, A. A. Ed.; Elsevier: Amsterdam, 1992; p 143.
(40) (a) Williams G. *Comprehensive Polymer Science*; Allen, G., Bevington, J. C. Eds.; Pergamon Press, 1989; Vol. II. (b) Williams, G. Structure and Properties of Polymers. In *Materials Science & Technology Series*; Thomas, E. L. Ed.; VCH: Weinheim, 1993; Vol *12*, p 471.
(41) Kresse, H. Dynamics in Thermotropic Calamitic Liquid Crystals Investigated by Dielectric Methods. *Modern Topics in Liquid Crystals. From Neutron Scattering to Ferroelectricity*; Buka, A. Ed.; World Scientific, 1993.
(42) *Handbook of Liquid Crystals*; Demus, D., Goodby, J., Gray, G. W., Spiess, H. W., Vill V. Eds.; Wiley-VCH: Weinheim, 1998.
(43) *Broadband Dielectric Spectroscopy*; Kremer, F., Schönhals, A. Eds.; Springer Verlag: Berlin, 2003.
(44) Brás, A. R.; Dionísio, M.; Huth, H.; Schick, Ch.; Schönhals, A. *Phys. Rev. E* **2007**, *75*, 061708.
(45) Capaccioli, S.; Prevosto, D.; Bets, A.; Hanewald, A.; Pakula, T. *J. Non-Cryst. Solids* **2007**, *353*, 4267.
(46) Van Boxtel, M. C. W.; Wübbenhorst, M.; Van Turnhout, J.; Bastiaansen, C. W. M.; Broer, D. J. *Liq. Cryst.* **2003**, *30*, 235.
(47) Brás, A. R. E.; Henriques, S.; Casimiro, T.; Aguiar Ricardo, A.; Sotomayor, J.; Caldeira, J.; Santos, C.; Dionísio, M. *Liq. Cryst.* **2007**, *34*, 591.
(48) Maschke, U.; Benmouna, M.; Coqueret, X. *Macromol. Rapid Commun.* **2002**, *23*, 159.
(49) Brás, A. R.; Viciosa, M. T.; Rodrigues, C.; Dias, C. J.; Dionisio, M. *Phys. Rev. E* **2006**, *73*, 061709.
(50) Roussel, F.; Buisine, J. M.; Maschke, U.; Coqueret, X. *Mol. Cryst. Liq. Cryst.* **1997**, *299*, 321.
(51) Anopore inorganic membranes are commonly used for laboratory filtration applications. More information can be obtained at www.whatman.com.
(52) Iannacchione, G. S.; Finotello, D. *Phys. Rev. Lett.* **1992**, *69*, 2094.
(53) Iannacchione, G. S.; Finotello, D. *Phys. Rev. E* **1994**, *50*, 4780.
(54) Jagadeesh, B.; Prabhakar, A.; Demco, D. E.; Buda, A.; Blümich, B. *Chem. Phys. Lett.* **2005**, *404*, 177.
(55) Kremer, F.; Schönhals, A. Broadband Dielectric Measurement Techniques. In *Broadband Dielectric Spectroscopy*; Kremer, F., Schönhals, A. Eds.; Springer Verlag: Berlin, 2003; p 35.
(56) Rózanski, S. A.; Stannarius, R.; Groothues, H.; Kremer, F. *Liq. Cryst.* **1996**, *20*, 59.
(57) Bengoechea, M. R.; Aliev, F. M. *J. Non-Cryst. Solids* **2005**, *351*, 2685.
(58) Vrbancic, N.; Vilfan, M.; Blinc, R.; Dolinsek, J.; Crawford, G. P.; Doane, J. W. *J. Chem. Phys.* **1993**, *98*, 3540.
(59) Zeng, H.; Finotello, D. *Phys. Rev. Lett.* **1992**, *69*, 2094.
(60) (a) Havriliak, S.; Negami, S. *Polymer* **1967**, *8*, 161. (b) Havriliak, S.; Negami, S. *J. Polym. Sci. C* **1966**, *16*, 99.
(61) Schönhals, A.; Kremer, F. Analysis of Dielectric Spectra. In *Broadband Dielectric Spectroscopy*; Kremer, F., Schönhals, A. Eds.; Springer Verlag: Berlin, 2003; p 59.
(62) Viciosa, M. T.; Nunes, A. M.; Fernandes, A.; Almeida, P. L.; Godinho, M. H.; Dionisio, M. *Liq. Cryst.* **2002**, *29*, 429.
(63) Sinha, G.; Aliev, F. *Phys. Rev. E* **1998**, *58*, 2001.
(64) Hourri, A.; Bose, T. K.; Thoen, J. *Phys. Rev. E* **2001**, *63*, 051702.
(65) Frunza, S.; Frunza, L.; Schönhals, A.; Tintaru, M.; Enache, I.; Beica, T. *Liq. Cryst.* **2004**, *31*, 913.
(66) Kremer, F.; Schönhals, A. The Scaling of the Dynamics of Glasses and Supercooled Liquids. In *Broadband Dielectric Spectroscopy*; Kremer, F., Schönhals, A. Eds.; Springer Verlag: Berlin, 2003; p 99.
(67) Kremer, F.; Schönhals, A. Molecular and Collective Dynamics of Polymeric. Liquid Crystals. In *Broadband Dielectric Spectroscopy*; Kremer, F., Schönhals, A. Eds.; Springer Verlag: Berlin, 2003; pp 392 ff.
(68) Kremer, F.; Huwe, A.; Schönhals, A.; Różañski, S. A. Molecular dynamics in Confining Space. In *Broadband Dielectric Spectroscopy*; Kremer, F., Schönhals, A. Eds.; Springer Verlag: Berlin, 2003; p 212.
(69) Lobo, C. V.; Prasad, S. K.; Rao, D. S. S. *Phys. Rev. E* **2004**, *69*, 051706.
(70) Schönhals, A.; Kremer, F. Theory of dielectric relaxation. In *Broadband Dielectric Spectroscopy*; Kremer, F., Schönhals, A. Eds.; Springer Verlag: Berlin, 2003; p 1.
(71) Steeman, P. A. M.; van Turnhout, J. Dielectric properties in Inhomogeneous Media. *Broadband Dielectric Spectroscopy*; Kremer, F., Schönhals, A. Eds.; Springer Verlag: Berlin, 2003.

JP802133E